Nuclear Engineering and Technology 52 (2020) 1481–1485

Contents lists available at ScienceDirect

Nuclear Engineering and Technology

journal homepage: www.elsevier.com/locate/net

Original Article

# Investigating creep behavior of Ni–Cr–W alloy pressurized tube at 950 °C by using in-situ creep testing system

Yang Zhong [a, b], Kuan-Che Lan [c], Hoon Lee [d], Bomou Zhou [e], Yong Wang [e], D.K.L. Tsang [e, *], James F. Stubbins [d, **]

[a] Department of Radiation Oncology, Fudan University Shanghai Cancer Center, Shanghai, China
[b] Department of Oncology, Shanghai Medical College, Fudan University, Shanghai, China
[c] Institute of Nuclear Engineering and Science, National Tsing Hua University, Hsinchu, 30013, Taiwan
[d] Department of Nuclear, Plasma, and Radiological Engineering, University of Illinois at Urbana-Champaign, Urbana, IL, 61801, USA
[e] Shanghai Institute of Applied Physics, Chinese Academy of Sciences (CAS), Shanghai, 201800, China

ARTICLE INFO

*Article history:*
Received 27 October 2019
Received in revised form
11 December 2019
Accepted 23 December 2019
Available online 25 December 2019

*Keywords:*
Ni-Cr-W alloy
Thermal creep
Finite element analysis

ABSTRACT

The creep behavior of Ni–Cr–W alloy at 950 °C has been investigated by a novel creep testing system which is capable of in-situ measurement of strain. Tubular specimens were pressurized with argon gas for effective stresses up to 32 MPa. Experimental results show that the thermal fatigue reduces the creep life of the tubular specimens and with the introduction of thermal cycling fatigue the primary stage disappears and the creep rate higher than the pure thermal creep (without thermal fatigue). Also the creep behavior of Ni–Cr–W alloy doesn't consist in the secondary stage. A new creep equation has been derived and implemented into finite element method. The results from the finite element analyses are in good agreement with the creep experiment.



## 1. Introduction

The very high temperature gas-cooled reactor is a promising Gen-IV nuclear system. Its designed temperature output can reach up to 950 °C, at which the efficiency of producing electricity and hydrogen will surpass the capabilities of current plants [1]. The intermediate heat exchanger (IHX) is a major component of the Very High Temperature Gas-cooled Reactor (VHTGR) and will be exposed to elevated temperatures and gas pressures up to 8 MPa [2,3]. Under these conditions, resistance to time-dependent deformation under sustained loading at elevated temperatures, or creep, is a major factor in lifetime performance and limits available materials for selection. Currently, a solid solution strengthened Ni–Cr–W Alloy 230 was considered to be one of the candidate structural materials for IHX tubing because of its excellent mechanical and corrosion resistance at elevated temperatures [4].

Creep deformation behavior Alloy 230 was investigated at various applied stresses from 750 °C to 950 °C [4–6]. It was found that the exhibition of the three classical creep regions (primary, secondary, and tertiary creep) depended on the applied stress and temperature. The primary and secondary stages of creep deformation were clearly observed under 0.10 yield strength stress exposure to 750 °C, 850 °C and 950 °C. At a higher stress level (0.25 yield strength), the tertiary stage appeared on early during creep strain development when the temperature was higher than 850 °C. Most of conventional creep tests were conducted using uniaxial cylindrical specimens as shown in Fig. 1(a). However, most of IHX design is tube-shaped structure in which the stress state is biaxial as shown in Fig. 1(b). Hence, the cylindrical specimens used in traditional creep tests do not represent well the real biaxial stress condition of in-service IHX components. Compared to uniaxial creep samples, the pressurized creep tube is a more efficient way to investigate creep behavior. This is because miniature configuration enables numerous tube-shaped samples loaded into a limited nuclear reactor at one time. Numerous studies have attempted to use pressurized tube for irradiation and creep testing for materials, which are exposed on multiple irradiation and high-temperature corrosive environments in reactor [7–10]. To investigate the biaxial thermal creep behavior of Inconel 617 and Alloy 230, Tung et al. [11] and Mo et al. [12] adapted the original design (Gilbert et al. [7]) of the creep tube for high -temperature creep tests. It was

* Corresponding author.
** Corresponding author.
*E-mail addresses:* DerekTsang@sinap.ac.cn (D.K.L. Tsang), jstubbin@illinois.edu (J.F. Stubbins).

https://doi.org/10.1016/j.net.2019.12.024

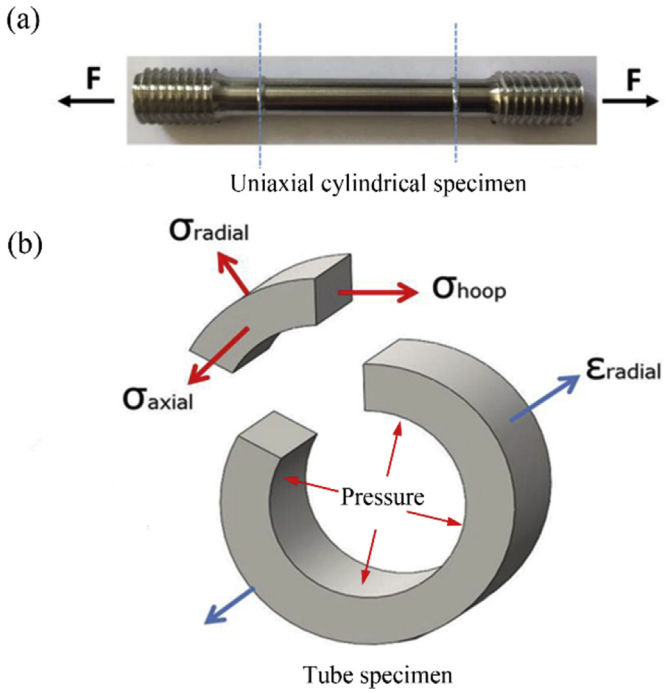


**Fig. 1.** Mechanical analysis of (a) uniaxial cylindrical specimen and (b) tube specimen.

found that for both alloys, tertiary creep accounts for a great portion of the materials' life, while secondary creep only accounts for a small portion. To provide estimation of creep life for a larger range of stresses and temperatures, a creep equation accurately representing the creep strain development of both alloy tubes has been derived in their work [11,12].

In the previous experiments, because of limitation of ex-situ experimental system, creep measurement data could only be obtained at the room temperature. Creep samples had to be cooled and removed from the furnace at selected time intervals for these measurements. These cooling and reheating processes results in temperatures gradients in testing samples. Repeated temperature gradients may introduce thermal fatigue [13]. Thermal fatigue is a critical life-limiting factor for many structure materials in high temperature applications. For example, the strains and stresses of reactor component vary between maximum and minimum values due to thermal fatigue. This is the main reason for the failure of structural components. Numerous studies have been devoted to better understand the effect of thermal fatigue on Ni-based alloys [14–22] Raffaitin et al. [15] demonstrated that for Nickel-based superalloy, thermal cycling creep rates are faster than isothermal creep rates. Vetriselvan et al. [22] also found that thermal fatigue causes tube (9Cr 1Mo steel) failures, significantly reducing the working life of the tubular components.

In the present paper, a new in-situ creep testing system has been developed to study the biaxial creep of tubular specimens. The diameter change of the specimens can be measured continuously in the new testing system. A schematic diagram and photograph of the key components of the in-situ creep testing system are illustrated in Fig. 2(a).

## 2. Materials and methods

The composition of the Alloy 230 used in this experiment is given in Table 1 from a certified test report (heat number: XX58A7UK). In contrast to the typical cylindrical specimens used in uniaxial creep test, pressurized tubes with an outside diameter of 4.5720 mm and wall thickness of 0.2540 mm were used in this investigation. The detailed dimensions of the specimen can be seen in Fig. 2(b) based on tube thermal creep analyses in Garner et al. [23]. Tubular specimens were pressurized with argon gas for effective stresses up to 32 MPa.The stress inside the tube can be determined by the middle wall effective stress, which is calculated based on von Mises criterion [24]:

$$\sigma_{eff} = \frac{\sqrt{3}R_0^2}{R_0^2 + R_m^2}\sigma_h \tag{1}$$

where $\sigma_h$ is given by

$$\sigma_h = \frac{PR_i^2}{R_0^2 - R_i^2}\left[1 + \frac{R_0^2}{R_m^2}\right] \tag{2}$$

$R_0$, $R_i$ and $R_m$ are the outer, inner, and mid-wall radii, respectively. P is the internal gas pressure.

Both ends of the specimens were welded using the electron

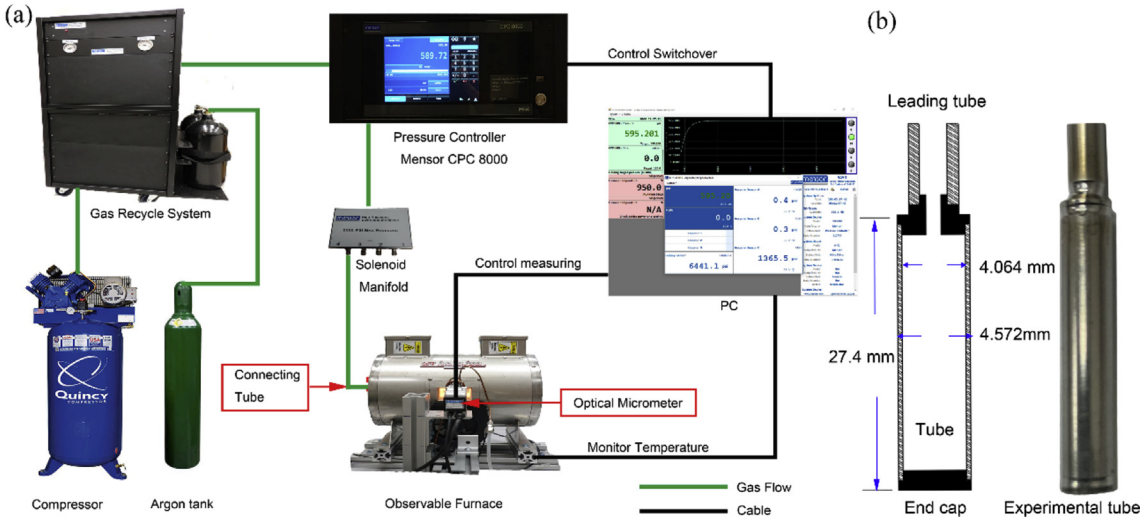


**Fig. 2.** (a) Schematic diagram of the in-situ creep system and (b) tubular specimen of Alloy 230.

**Table 1**
Chemical composition of Alloy 230 for tube specimens (weight%).

| Al | B | C | Co | Cr | P | Fe |
|---|---|---|---|---|---|---|
| 0.37 | 0.03 | 0.11 | 0.19 | 22.39 | 0.008 | 1.55 |
| Mn | Mo | Ni | S | Si | Ti | W |
| 0.5 | 1.36 | BAL | 0.02 | 0.38 | 0.01 | 14.26 |

**Table 2**
The rupture time compared with Tung's experiment of Alloy 230 at 950 °C [11].

| Effective Stress (MPa) | Ex-situ system (hours) | In-situ system (hours) | In-situ/Ex-situ ratio |
|---|---|---|---|
| 23 | 115 | 216 | 1.88 |
| 18 | 237 | 410 | 1.73 |

beam welding technique, which can reduce the defects that might induce early rupture. Before exposure of specimen in the test environment, the sealed tube was purged six times in order to minimize the oxidation of the inner wall when the specimen was inserted into the furance. The outer surface of creep tubes was exposed to air at 950 °C. The furnace was then heated to the working temperature, followed by 30 min stabilization of the temperature. High purity argon gas (99.998%) was employed to pressurize the specimens, and the gas pressure was controlled and monitored by a pressure controller, Mensor CPC8000. The outer diameter at the middle of the pressurized creep tubes was measured each second during the experiments by optical micrometer. After rupture, the specimen was vented, and withdrawn out of furnace.

## 3. Results and discussion

To examine the thermal fatigue behavior on tube-shape Alloy 230 specimens, creep tests of the Alloy 230 pressurized tubes without thermal fatigue effect under the same testing conditions and heat number as in Tung [11] were conducted using the new in-situ testing system. The results are listed in Table 2 and compared with Tung's data. It can be seen that the rupture times in present experiment are significantly longer than in Tung's work, which indicates the ex-situ measurement may include the thermal-fatigue damage in the creep life estimation, and can be more conservative compared to the in-situ creep strain measurement where the creep tube deforms continuously. The deteriorated effect of thermal cycling fatigue present in ex-situ biaxial creep test at elevated temperature is significant and should be avoided. It is postulated that the ex-situ system experiments would predict much shorter creep life at comparable effective stress levels than the in-situ system.

The creep strain curves of Alloy 230 at different pressures from 18 MPa to 32 MPa at 950 °C is shown in Fig. 5(b). It can be seen that the ruptured times of the tubular specimens have a strong relationship to applied pressure and the time to failure dramatically decreases with increasing of applied pressure.

To evaluate the thermal cycling fatigue effect, creep experiments coupled with thermal-fatigues were designed. In contrast to the conventional creep experiments, the specimens were cooled to ambient temperature after 1-h and 4-h isothermal exposure. They then reinserted in the furnace for a second exposure, and this process was repeated until the end of the creep life. Fig. 3(a) shows the diameter strain development of Alloy 230 with pure creep, 1-h and 4-h interval creep under the pressure 32 MPa at 950 °C. It can be observed that the thermal cycling fatigue reduces the creep life of the tube and the frequency of thermal cycling has little influence on creep life. To further determine the impact of thermal cycling fatigue on the three classical creep regions (primary, secondary, and tertiary creep), the creep strain rate curves are depicted in Fig. 3(b). It illustrates that with the introduction of thermal cycling fatigue the primary stage disappears and the creep rate higher than the pure creep.

To determine whether the alloy exhibited three classical creep regions (primary, secondary, and tertiary creep) with respect to applied stress, Fig. 4 shows the creep strain rate plotted as a function of the average strain on a semi-log scale. It can be seen that the tertiary creep takes a greater portion of all these curves and it occurs early during the test without secondary creep, which is consistent with the previous study [11]. Similar results have been observed for Ni-based alloy under an applied uniaxial stress state, including Inconel 738 alloy [25], Inconel 617 alloy [12] and 718 alloy [26].

As we mentioned above, the steady creep state is not present in Alloy 230 creep behavior at 950 °C. Hence, it is necessary to develop a suitable constitutive equation which fit the above experimental data and can describe the creep stages accurately and represent the biaxial stress distribution of pressured tube. Previously, Gilbert and Blackburn [10] have formulated a creep equation in the form:

$$\varepsilon_c = A\sigma_{eff}\cosh^{-1}(1+Bt) + C\sigma_{eff}^{n}t^{m} + D\sigma_{eff}^{n}t^{2.5} \tag{3}$$

where $\varepsilon_c$ is the creep strain, $t$ is the time and the remaining quantities are temperature dependent parameters. The equation (3) can accurately represent the creep strain behavior of 316 stainless steel creep tubes which contains a linear dependence of the creep strain on stress at low stress levels with a much stronger

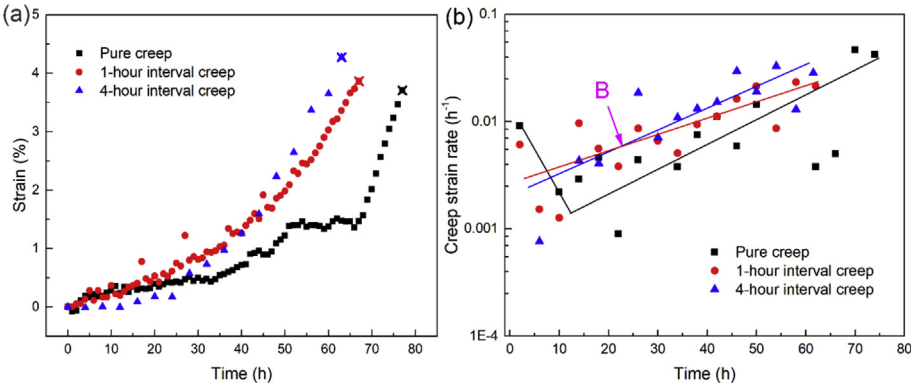


**Fig. 3.** Conventional creep test at loading 32 MPa, 1-h and 4-h interval creep of alloy 230 at 950 °C (a) creep curves and (b) creep strain rate.

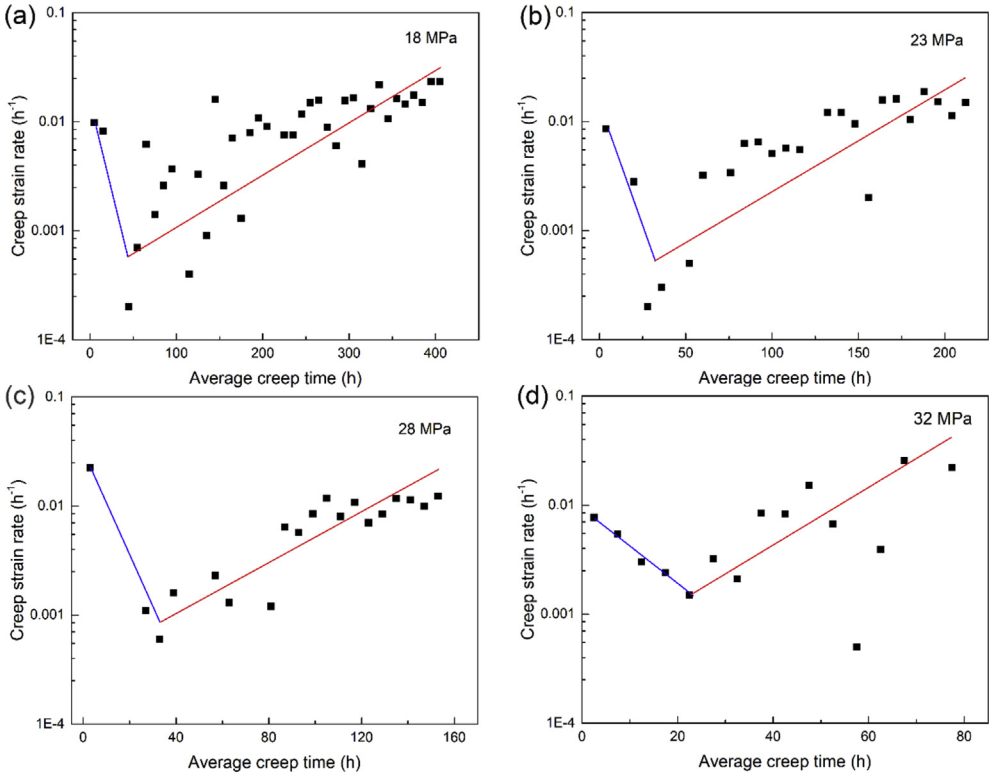


**Fig. 4.** Creep strain rate for Alloy 230 at 950 °C with applied stress of (a) 18 MPa, (b) 23 MPa, (c) 28 MPa and (d) 32 MPa. The blue and red lines in the figures represent primary and tertiary creep, respectively. (For interpretation of the references to colour in this figure legend, the reader is referred to the Web version of this article.)

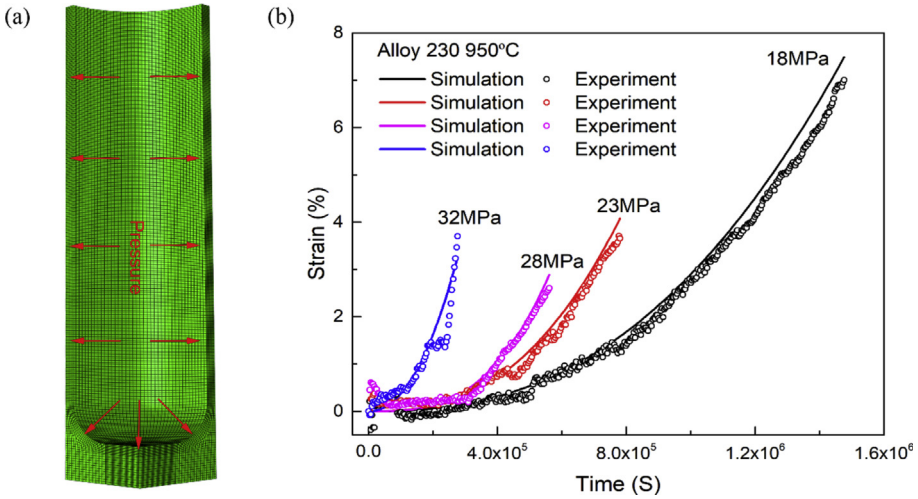


**Fig. 5.** (a) 1/8 finite element model for pressurized creep tube, (b) Comparison of experimental results with finite element analyses of Alloy 230 at 950 °C with effective stresses of 18 MPa, 23 MPa, 28 MPa and 32 MPa.

stress dependence appearing at higher stress levels. For Alloy 230 and 617 tubes, Mo et al. [12] have modified equation (3) to fit their experimental results and creep strain becomes:

$$\varepsilon_c = A\sigma_{eff}\cosh^{-1}(1+Bt) + C\sigma_{eff}^{n}t^{m} \quad (4)$$

The creep equation (4) can adequately represent the results of the biaxial creep strain development for Alloy 230, particularly in high and medium stresses. However, for lower stresses the computed creep curves do not fit well to the experimental results [12]. The deviation for low stresses is attributed to the deficiency of long-term creep data, which influences the accuracy of fitting between experimental data and the creep equation. This is an obstacle to the development of a better sets of temperature-dependent constants and stress-dependent constants.

The in-situ measurement system used in this study can provide more accuracy creep data to fit the parameters in equation (4) to reduce the deviation at low stress levels. Furthermore, the value of

**Table 3**
Values of exponent in the creep equation for Alloy 230 at different effective stresses.

| Alloy 230 | 18 MPa | 23 MPa | 28 MPa | 32 MPa |
|---|---|---|---|---|
| n | 1.32 | 1.37 | 1.39 | 1.5 |

*n* in creep equation not only be regarded as a temperature parameter as in Mo et al. [12] and Gilbert et al. [10] but also as pressure-dependent parameter. Table 3 shows the values of n at different effective stresses. As you can see from the table the value of *n* is a function of effective stress, increasing moderately with the stress level.

A finite element model which represents one-eighth of creep tubular specimen is shown in Fig. 5(a). The model was used to verify the creep test results and the creep equation (4). The finite element model has 560,090 nodes and 129,000 elements. 8-noded tetrahedral reduced integral three-dimensional solid element was used in finite element analyses. equation (4) has been implemented into commercial FE solver ABAQUS via a user-defined subroutine CREEP. The creep tests have been simulated at 950 °C with four effective stresses (18 MPa, 23 MPa, 28 MPa and 32 MPa). The parameters in equation (4) are fitted according to creep test results.

The experimental and finite element results are plotted together in Fig. 5(b) showing good agreement between the results of the experiments and finite element analyses. This newly derived creep equation (4) could be extended to a large range stress to estimate creep life and understand the creep properties of Alloy 230. In addition the creep equation can be used to assess the structural integrity of components at elevating temperature.

## 4. Conclusions

In summary, a new in-situ creep system was built to carry out creep tests for tubular specimens and to examine the biaxial creep behavior of Alloy 230 at 950 °C under effective stress of 18 MPa, 23 MPa, 28 MPa and 32 MPa. The main findings from these creep tests are listed below:

1. Thermal cycling fatigue reduces the creep life of the tube-shap creep specimens and, with the introduction of thermal cycling fatigue, the primary stage disappears accompanied by a higher creep rate than pure thermal creep.
2. The creep curves are mainly composed of a primary stage and a larger percentage tertiary stage without a significant steady-state creep stage. The tertiary regime takes a greater fraction of creep life.
3. A creep equation was developed based on biaxial creep data and implemented into finite element method via a user-defined subroutine to simulate creep behavior of pressurized tubular specimen. The experimental data and the results of finite element method are in close agreement with each other.

## Declaration of competing interest

The authors declare that they have no known competing financial interests or personal relationships that could have appeared to influence the work reported in this paper.

## Acknowledgements

The authors would like to acknowledge the financial support from the Strategic Priority Research Program of the Chinese Academy of Sciences (No. XDA02040000). Thanks for the funding support from the China Scholarship Council for 1-year study at the University of University of Illinois at Urbana-Champaign and National Natural Science Foundation of China (Grant No. U1632268).

## Appendix A. Supplementary data

Supplementary data to this article can be found online at https://doi.org/10.1016/j.net.2019.12.024.

## References

[1] D. Chapin, S. Kiffer, J. Nestell, The Very High Temperature Reactor: A Technical Summary, MPR Associates, Inc, Alexandria, 2004.
[2] W.R. Corwin, T. Burchell, W. Halsey, G. Hayner, Y. Katoh, J. Klett, T. McGreevy, R. Nanstad, W. Ren, L. Snead, Updated Generation IV Reactors Integrated Materials Technology Program Plan, 2004. ORNL/TM-2003/244 1.
[3] W. Ren, R. Swindeman, A review on current status of alloys 617 and 230 for Gen IV nuclear reactor internals and heat exchangers, J. Press. Vessel Technol. 131 (4) (2009), 044002.
[4] S. Chatterjee, A.K. Roy, Mechanism of creep deformation of Alloy 230 based on microstructural analyses, Mater. Sci. Eng. A 527 (29–30) (2010) 7893–7900.
[5] C. Boehlert, S. Longanbach, A comparison of the microstructure and creep behavior of cold rolled HAYNES® 230 alloy™ and HAYNES® 282 alloy™, Mater. Sci. Eng. A 528 (15) (2011) 4888–4898.
[6] J. Yoon, H. Jeong, Y. Yoo, H. Hong, Influence of initial microstructure on creep deformation behaviors and fracture characteristics of Haynes 230 superalloy at 900° C, Mater. Char. 101 (2015) 49–57.
[7] E. Gilbert, J. Bates, Dependence of Irradiation Creep on Temperature and Atom Displacements in 20% Cold Worked Type 316 Stainless Steel, Measurement of Irradiation-Enhanced Creep in Nuclear Materials, Elsevier1977, pp. 204-209.
[8] J. Vitek, D. Braski, J. Horak, Effect of preinjected helium on the response of V-20Ti pressurized tubes to neutron irradiation, J. Nucl. Mater. 141 (1986) 982–986.
[9] H. Tsai, H. Matsui, M. Billone, R. Strain, D. Smith, Irradiation creep of vanadium-base alloys, J. Nucl. Mater. 258 (1998) 1471–1475.
[10] E. Gilbert, L. Blackburn, Creep deformation of 20 percent cold worked type 316 stainless steel, J. Eng. Mater. Technol. 99 (2) (1977) 168–180.
[11] H.-M. Tung, K. Mo, J.F. Stubbins, Biaxial thermal creep of Inconel 617 and haynes 230 at 850 and 950° C, J. Nucl. Mater. 447 (1–3) (2014) 28–37.
[12] K. Mo, W. Lv, H.-M. Tung, D. Yun, Y. Miao, K.-C. Lan, J.F. Stubbins, Biaxial thermal creep of alloy 617 and alloy 230 for VHTR applications, J. Eng. Mater. Technol. 138 (3) (2016), 031015.
[13] R. Viswanathan, Damage Mechanisms and Life Assessment of High Temperature Components, ASM international, 1989.
[14] J. Zhang, Y. Ro, H. Zhou, H. Harada, Deformation twins and failure due to thermo-mechanical cycling in TMS-75 superalloy, Scr. Mater. 54 (4) (2006) 655–660.
[15] A. Raffaitin, D. Monceau, F. Crabos, E. Andrieu, The effect of thermal cycling on the high-temperature creep behaviour of a single crystal nickel-based superalloy, Scr. Mater. 56 (4) (2007) 277–280.
[16] J. Zhang, H. Harada, Y. Ro, Y. Koizumi, T. Kobayashi, Thermomechanical fatigue mechanism in a modern single crystal nickel base superalloy TMS-82, Acta Mater. 56 (13) (2008) 2975–2987.
[17] J. Zhang, H. Harada, Y. Koizumi, T. Kobayashi, Crack appearance of single-crystal nickel-base superalloys after thermomechanical fatigue failure, Scr. Mater. 61 (12) (2009) 1105–1108.
[18] J. Cormier, M. Jouiad, F. Hamon, P. Villechaise, X. Milhet, Very high temperature creep behavior of a single crystal Ni-based superalloy under complex thermal cycling conditions, Philos. Mag. Lett. 90 (8) (2010) 611–620.
[19] B. Fu, J. Zhang, H. Harada, Significant thinning of deformation twins and its effect on thermomechanical fatigue fracture in nickel base single crystal superalloys, Mater. Sci. Eng. A 605 (2014) 253–259.
[20] F. Sun, J. Zhang, H. Harada, Deformation twinning and twinning-related fracture in nickel-base single-crystal superalloys during thermomechanical fatigue cycling, Acta Mater. 67 (2014) 45–57.
[21] C. Panwisawas, N. D'Souza, D.M. Collins, A. Bhowmik, B. Roebuck, History dependence of the microstructure on time-dependent deformation during in-situ cooling of a nickel-based single-crystal superalloy, Metall. Mater. Trans. A 49 (9) (2018) 3963–3972.
[22] R. Vetriselvan, P. Sathiya, G. Ravichandran, Experimental and numerical investigation on thermal fatigue behaviour of 9Cr 1Mo steel tubes, Eng. Fail. Anal. 84 (2018) 139–150.
[23] F. Garner, M. Hamilton, R. Puigh, C. Eiholzer, D. Duncan, M. Toloczko, A. Kumar, The Influence of Specimen Size on Measurement of Thermal or Irradiation Creep in Pressurized Tubes, Effects of Radiation on Materials: Sixteenth International Symposium, ASTM International, 1994.
[24] G.M. Timoshenko P, W. Prager, Theory of Elastic Stability, 1962.
[25] G. Jianting, D. Ranucci, E. Picco, P. Strocchi, An investigation on the creep and fracture behavior of cast nickel-base superalloy IN738LC, Metallurgical Transactions A 14 (11) (1983) 2329–2335.
[26] K. Chen, J. Dong, Z. Yao, T. Ni, M. Wang, Creep performance and damage mechanism for Allvac 718Plus superalloy, Mater. Sci. Eng. A 738 (2018) 308–322.